Journal of the American Statistical Association

ISSN: 0162-1459 (Print) 1537-274X (Online) Journal homepage: http://www.tandfonline.com/loi/uasa20

Forecasting Generalized Quantiles of Electricity Demand: A Functional Data Approach

Brenda López Cabrera & Franziska Schulz

To cite this article: Brenda López Cabrera & Franziska Schulz (2017) Forecasting Generalized Quantiles of Electricity Demand: A Functional Data Approach, Journal of the American Statistical Association, 112:517, 127-136, DOI: 10.1080/01621459.2016.1219259

To link to this article: https://doi.org/10.1080/01621459.2016.1219259

JOURNAL OF THE AMERICAN STATISTICAL ASSOCIATION
2017, VOL. 112, NO. 517, 127–136, Applications and Case Studies
http://dx.doi.org/10.1080/01621459.2016.1219259

Taylor & Francis
Taylor & Francis Group

Forecasting Generalized Quantiles of Electricity Demand: A Functional Data Approach

Brenda López Cabrera and Franziska Schulz

Ladislaus von Bortkiewicz Chair of Statistics, Humboldt-Universität zu Berlin, Berlin, Germany

ABSTRACT

Electricity load forecasts are an integral part of many decision-making processes in the electricity market. However, most literature on electricity load forecasting concentrates on deterministic forecasts, neglecting possibly important information about uncertainty. A more complete picture of future demand can be obtained by using distributional forecasts, allowing for more efficient decision-making. A predictive density can be fully characterized by tail measures such as quantiles and expectiles. Furthermore, interest often lies in the accurate estimation of tail events rather than in the mean or median. We propose a new methodology to obtain probabilistic forecasts of electricity load that is based on functional data analysis of generalized quantile curves. The core of the methodology is dimension reduction based on functional principal components of tail curves with dependence structure. The approach has several advantages, such as flexible inclusion of explanatory variables like meteorological forecasts and no distributional assumptions. The methodology is applied to load data from a transmission system operator (TSO) and a balancing unit in Germany. Our forecast method is evaluated against other models including the TSO forecast model. It outperforms them in terms of mean absolute percentage error and mean squared error. Supplementary materials for this article are available online.

ARTICLE HISTORY
Received June 2014
Revised June 2016

KEYWORDS
Expectiles; FPCA; Functional time series; Short-term load forecasting

1. Introduction

With the liberalization of energy markets, the amount of risk borne by operators and market participants has increased substantially. Statistical tools can be beneficial to assess and manage their risk. Among energy, electricity stands out due to its limited storability. Supply and demand have to be balanced out at every point in time. Since electricity is mainly traded in a day-ahead market, short-term adjustments in supply due to forecasting errors can lead to enormous financial losses. Therefore, load forecasting is extremely important for energy suppliers, transmission system operators, financial institutions, and other participants in electricity markets and a crucial process in the planning and operation of electric utilities.

There is a vast literature on how to forecast electricity load, most of them concentrating on deterministic forecasts. For an overview on common methods see Weron (2007) or Taylor and McSharry (2007). However, for a sustainable risk management of utility operators not only a forecast of expected demand, but also knowledge of the uncertainty and dispersion of future load plays an important role. This points toward the use of probabilistic forecasts. While in different areas of forecasting such as macro-economics and finance (Tay and Wallis 2000), meteorology (Leutbecher and Palmer 2008), and renewable energy production (Bremnes 2004; Pinson, Chevallier, and Kariniotakis 2007) probabilistic forecasts are already well established, there is a lack in literature on probabilistic forecasts for electricity demand. A notable exception is the work by Hyndman and Fan (2010), which uses a mixture of temperature simulation, economic scenarios, and residual bootstrapping to obtain long-term density forecasts of electricity demand. Others like Cottet and Smith (2003) use Bayesian modeling in a multi-equation regression model to forecast intraday electricity load and briefly discuss model averaging for probabilistic forecasts.

Short-term probabilistic forecasts yield important information for utility operators for decisions, for example, on purchasing and generating electricity and load scheduling. They are crucial for risk management and can be used to derive risk measures such as probability of exceedance levels (Taylor 2008; Bellini et al. 2014). In this article, we propose a methodology to obtain probabilistic forecasts by employing functional data analysis of generalized quantile curves.

With generalized quantiles we refer to quantiles (Koenker and Bassett Jr 1978) and expectiles (Newey and Powell 1987). Both are tail measures and uniquely characterize the conditional distribution of a random variable. They depend on an asymmetry parameter $\tau \in (0, 1)$ determining which part of the distribution they describe, where $\tau = 0.5$ corresponds to the central part of the distribution, while generalized quantiles with small and large values of τ describe the tails of the distribution. Furthermore, for a large class of decision-making problems, optimal solutions correspond to quantiles of a conditional predictive distribution (Gneiting 2011). In fact, in a wide range of fields including weather events, extreme natural hazards, genomics, risk management, energy demand, and portfolio allocation among others, tail indices provide useful information that goes beyond the mean and median. These tail indices

CONTACT Franziska Schulz sulzfran@hu-berlin.de Ladislaus von Bortkiewicz Chair of Statistics, Humboldt-Universität zu Berlin, Spandauer Straße 1, 10178 Berlin, Germany.
Color versions of one or more of the figures in the article can be found online at www.tandfonline.com/r/JASA.
Supplementary materials for this article are available online. Please go to www.tandfonline.com/r/JASA.

constitute curves that can be treated in a functional principal component analysis (FPCA) context.

The idea of FPCA is to identify the main risk drivers by a small number of factors combined with random noise. The resulting factors are then to be (cor)related with exogenous variables, which will allow us to study phenomena contingent to extreme risks. Functional data analysis (see Ramsay and Silverman 2005) is an extension of multivariate data analysis to functional data. There are few studies that apply methods from functional data analysis to load forecasting, among them Shang (2013), Goia, May, and Fusai (2010), and Antoch et al. (2008). A significant contribution is Liebl (2013), who introduces a functional factor model to forecast daily price-demand functions. Vilar, Cao, and Aneiros (2012) applied functional nonparametric and semifunctional partial linear models to obtain day-head forecasts of electricity demand and prices. A nonparametric functional model is also applied by Aneiros et al. (2011), who derived bidding strategies from residual demand forecasts. Ferraty et al. (2014) proposed a semiparametric functional model with functional predictors and scalar response to forecast daily peak load. Others like Cho et al. (2013) reduced dimension using a hybrid approach that combines a generalized additive model for the weekly averages of the load and curve linear regression models for the dependence structure across consecutive daily loads.

Two recent studies on functional data analysis of tail events are Guo et al. (2015), who do the dimension reduction with weighted L_1 and L_2 norm, where the weights are sign sensitive, and Tran, Osipenko, and Härdle (2016) who developed an analog of PCA of tail curves in an asymmetric norm. However, both studies rely on independence between functional observations. In many fields however, including energy demand modeling, the dependency between curves needs to be taken into account at the core of the modeling. In our study, we allow for temporal dependence between functional observations and refer to results from Hörmann and Kokoszka (2010). A comprehensive overview of methods for dependent functional data is given by Horváth and Kokoszka (2012). The dependence between tail curves can be exploited for forecasting, which provides useful information to support modeling, pricing, and trading. Our approach has several advantages: It allows for flexible inclusion of explanatory variables and does not require distributional assumptions for the tails curves. Furthermore, treating load curves as functional data has the advantage that one step ahead forecasts yield forecasts for the whole next day and that forecasts are continuous functions and thus available on an arbitrarily fine grid. Forecasts of single generalized quantiles provide, depending on the chosen quantile level, information about expected demand and risk measures such as probability of exceedance levels. Forecasts of a collection of generalized quantile curves characterize the distribution of future electricity demand and therefore, provide a more complete picture than point forecasts. We expect that exogenous variables like meteorological factors do not only affect the amount of electricity consumed, but also influence the distribution over the day and thus the shape of the load curves (Engel et al. 1986; Harvey and Koopman 1993; Taylor and McSharry 2007).

We illustrate our approach with data on quarter-hourly electricity consumption of a transmission system operator (TSO) and a balancing unit (BU) in western Germany. Variations in the intradaily pattern are explained using weather variables and meteorological forecasts. The proposed model is shown to perform better than well-known methods, such as a deterministic similar-day approach, the Holt–Winter Exponential smoothing, and the forecast provided by TSO Amprion. On average it achieves 2.7% mean absolute percentage error (MAPE) in the one-day forecasting period of the mean for the TSO.

Our article is structured as follows. Section 2 gives a brief introduction of the load data. In Section 3, we define FPCA of generalized quantiles that will be used to produce probabilistic load forecasts, together with its estimation algorithm. Section 4 discusses the modeling and estimation of the electricity demand data. Section 5 describes the forecast performance with respect to other methods and evaluates the probabilistic forecasts. Section 6 concludes the article. All computations in this article were carried out in R. The electricity load data and forecast electricity load data were obtained from TSO Amprion and the balancing unit Stadtwerke Saarbrücken. The data source for the temperature data is Deutscher Wetterdienst (DWD); for the meteorological weather forecast data the data source is WeatherOnline. We thank Dr. Ulrich Römer and Herrad Werner for providing us the data. To simplify notation, in the following dates are denoted in the yyyymmdd format.

2. Electricity Demand Data

The German electricity market, which was liberalized in 1998, is Europe's largest, with an annual power consumption of around 500 TWh and a generation capacity of 125 GW (Eurostat 2014). The four German TSOs (Amprion, Tennet TSO, 50 Hertz Transmission, and TransnetBW) are responsible for maintaining a stable and reliable system and to maintain balance between electricity generation and consumption. All market participants are organized in balancing units (BU). Each BU has a BU manager, responsible for the balance within the unit. Electricity is to a large extent traded in the day-ahead market, which closes daily at 12 p.m. Before market closure, each BU manager is required to submit a load schedule to the corresponding TSO specifying the expected load for each quarter-hour of the next day. Deviations from the specified load can still be adjusted in the intraday market. The intraday market is a continuous market where contracts can be traded until 15 min before delivery. Although the intraday market has been growing recently, it still plays a minor role in terms of trading volume. In 2013, the trading volume in the intraday market was only 8% of the trading volume in the day-ahead market (EPEX Spot 2014). Furthermore, prices in the intraday market are usually higher and more volatile than prices in the day-ahead market (Mayer 2014), making it rewarding to buy electricity in the day-ahead market. Therefore, we neglect the intraday market in this study.

The TSOs balance out differences between the forecasted load of the BU and actual consumption to ensure a stable system.

Table 1. Summary statistics of the load data (in MW).

	Median	Mean	SD	Min	Max
TSO	22,017	22,048	4052.68	11,854	34,868
BU	402	401	95.71	152	630

Precise forecasts of the area's consumption are essential to have sufficient capacity available. For deviations between forecasted and actual load, BUs have to pay a price that usually greatly exceeds the price at the spot market. Therefore, for BU managers improvements in their forecasting performance directly leads to cost reductions.

For the empirical work of this article, we use electricity demand data of the TSO Amprion and the BU Stadtwerke Saarbrücken. Both datasets are freely accessible on their websites. The TSO Amprion operates in western Germany. The BU is located within the balancing area of Amprion. The analysis is based on quarter-hourly data of electricity consumption from 20100101 to 20123112. Summary statistics are given in Table 1. The first two years of the data are used for in-sample fitting and the third year for an out-of-sample forecasting evaluation, given in Section 5. Figure 1 displays the two load datasets from 2010 to 2012. It is clearly visible that electricity consumption exhibits seasonal features over time and at different times of the day. It contains annual, weekly, and intraday seasonal cycles and is sensitive to temperature changes (Engel et al. 1986; Taylor and Buizza 2002). During winter electricity consumption in Germany is higher than during the summer. Additionally, at weekends electricity consumption is usually lower than during the week. The typical intraday load profile shows a peak around noon, followed by valley in the afternoon and another peak in the evening at around 7 p.m. Typical load curves for high and low demand days together with estimates of expectiles (generalized quantiles) corresponding to various levels of asymmetry τ (see definition in Section 3.1) are shown in Figure 2. While the expected value ($\tau = 0.5$) is a good point estimate, the range of expectile estimates yields information about uncertainty and dispersion of electricity demand.

The seasonal patterns of the load curves are quite predictable and therefore usually modeled deterministically. We express the observed load $\tilde{Y}_s$ as

$$\tilde{Y}_s = \Lambda_s + Y_s, \qquad s = 1, \dots, S, \tag{1}$$

where Λ_s is a deterministic seasonal component and Y_s is a stochastic component. We estimate the deterministic seasonal component separately for every quarter-hour of a day. It is specified as

$$\Lambda_{t,k} = a_t + b_t \cdot k + c_{1,t} \sin\left(\frac{2\pi k}{365}\right) + c_{2,t} \cos\left(\frac{2\pi k}{365}\right) + \sum_{i=1}^{7} d_{i,t} \cdot D_{i,k}, \tag{2}$$

where $t = 1, \dots, T$ denotes the quarter-hours of a day and $k = 1, \dots, N$ the day, such that $T = 96$ and $T \cdot N = S$. The parameters a_t, b_t, $c_{1,t}$, $c_{2,t}$, and $d_{i,t}$ are estimated by ordinary least-square regression. $D_{i,k}$ is a set of dummy variables consisting of six dummies for the weekdays and one dummy for public holidays. They capture weekly seasonal behavior, while the sine and cosine functions capture yearly seasonalities. This approach is very close to the so-called similar-day approach, which is a commonly used approach in industry to model and forecast electricity load.

As covariates for load modeling, we include average daily temperature and daily hours of sunshine. The time series of both variables are displayed in Figure 3. For Saarbrücken temperature and hours of sunshine are measures from a weather station

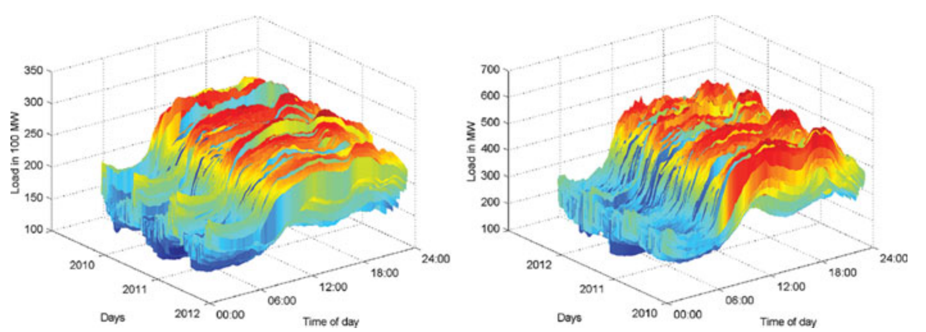

Figure 1. Electricity load curves of TSO Amprion (left) and BU Stadtwerke Saarbrücken (right) from 20100101 to 20123112.

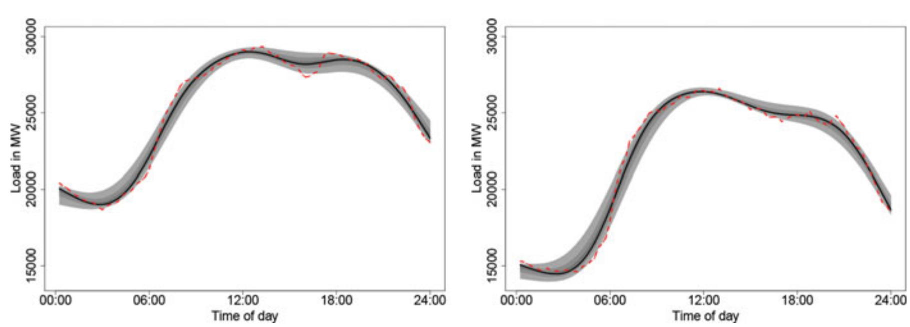

Figure 2. Observed load (red dashed line) for TSO Amprion together with estimates of the expected load (black solid line) and of expectiles corresponding to level of asymmetry $\tau = 0.01; 0.05; 0.25; 0.75; 0.95; 0.99$ (gray shades) on a high demand day 20101220 (left) and on a low demand day 20110912 (right).

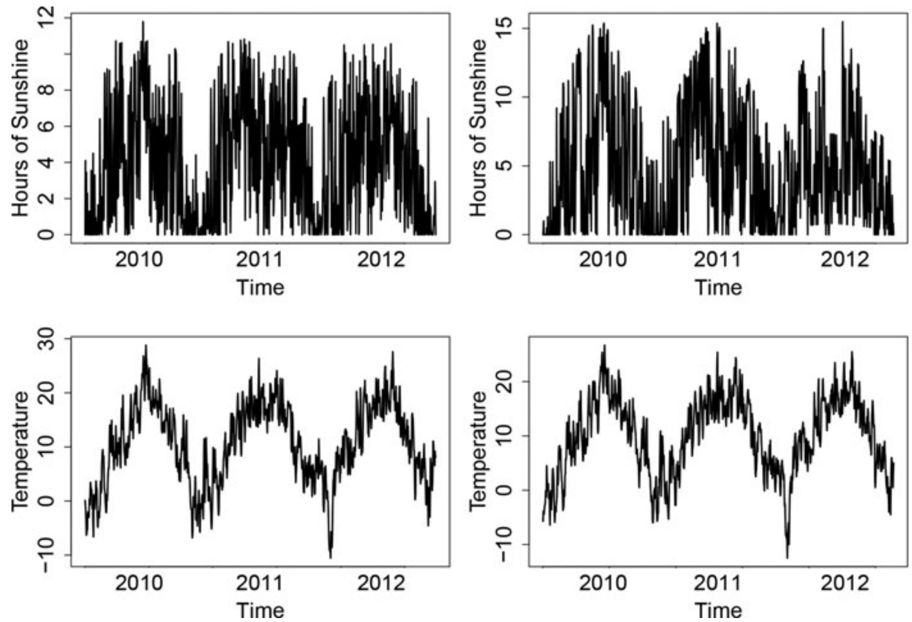

Figure 3. Average daily temperature and hours of sunshine for the area of the TSO Amprion (left) and Saarbrücken (right).

in Saarbrücken. For the TSO, the average measures of three stations located in their area are taken. For forecasting, we use meteorological day-ahead forecasts of the covariates, which are provided by WeatherOnline. For our analysis all covariates are deseasonalized.

3. Methodology

We propose a methodology that combines methods from generalized quantile regression and functional data analysis (FDA) to obtain probabilistic forecasts of electricity demand. FDA has gained importance with the advances in storing large sets of multivariate data. It has been applied in various fields of research ranging from bioscience to medicine and econometrics. For an overview on applications of FDA, we refer to Ramsay and Silverman (2002) and Ferraty and Vieu (2006).

3.1. Generalized Quantiles

The distribution of a random variable Y can be characterized by its cdf $F_Y(y)$. The quantile functions of Y are defined as

$$Q_Y(\tau) = F_Y^{-1}(\tau) = \inf\{y : F(y) \leq \tau\}, \qquad \tau \in (0, 1). \quad (3)$$

Like the cdf, the quantile function provides a full characterization of the random variable Y. For each $\tau \in (0, 1)$, the quantile function can be formulated as the solution of a minimization problem:

$$Q_Y(\tau) = \arg\min_y \mathrm{E}\{\rho_\tau(Y - y)\}, \quad (4)$$

where $\rho_\tau(\cdot)$ is a loss function defined as

$$\rho_\tau(u) = u\{\tau - \mathrm{I}(u < 0)\}, \quad (5)$$

which is in general asymmetric (Koenker 2005). A special case is the median, which corresponds to $\tau = 0.5$. The quantile function conditional on a (one-dimensional) covariate X is given by

$$Q_{Y|X}(\tau) = \arg\min_{f \in \mathcal{F}} \mathrm{E}\{\rho_\tau(Y - f(X))\}, \quad (6)$$

where $f(\cdot)$ is a nonparametric function of the covariate X from a set of functions $\mathcal{F}$, such that the expectation is well defined. Closely related to quantiles are expectiles introduced by Newey and Powell (1987), which can be obtained by a generalization of the loss function $\rho_\tau(\cdot)$:

$$l_\tau(X) = \arg\min_{f \in \mathcal{F}} \mathrm{E}\left\{\rho_\tau^\alpha(Y - f(X)\right\}, \qquad \alpha \in \{1, 2\} \quad (7)$$

$$\rho_\tau^\alpha(u) = |u|^\alpha|\tau - \mathrm{I}(u < 0)|. \quad (8)$$

We call the solution of (7) a generalized quantile function. For $\alpha = 1$, we obtain the loss function in (5) and the solution to (7) is a conditional quantile function. For $\alpha = 2$, the solution to (7) is a conditional expectile function. Note that the conditional expectile corresponding to $\tau = 0.5$ is the expected value $\mathrm{E}(Y|X)$. Like quantiles, expectiles characterize the distribution of a random variable. The interpretation of expectiles is as follows. While the τ-quantile is determined such that $\tau \cdot 100\%$ of the observations lie below the quantile, expectiles take into account how far the observations lie below the expectile. That is, the τ-expectile is determined such that $\tau \cdot 100\%$ of the distance of observations to the expectile corresponds to observations below the expectile. Moreover, expectiles are in fact quantiles of a distribution G related to F as shown by Jones (1994). While expectiles are less intuitive to interpret than quantiles, they have the advantage of a better computational efficiency (Newey and Powell 1987) and are a coherent risk measure (Bellini et al. 2014).

If one is not only interested in estimating a single generalized quantile, but in estimating a whole collection of generalized quantiles, one faces the problem of crossing quantiles/expectiles. This is unfavorable, since it is theoretically impossible. We use an algorithm proposed by Schnabel (2011), which estimates the generalized quantile functions jointly as a surface on the domain of the independent variable X and the asymmetry parameter τ, called expectile sheet. The expectile sheet can be expressed as

$$l(X,\tau) = \sum_{i=1}^{I}\sum_{j=1}^{J} a_{ij}B_i(X)\tilde{B}_j(\tau), \tag{9}$$

where $B_i(X)$ are B-Spline basis functions on the domain of the covariate X, $\tilde{B}_j(\tau)$ are B-spline basis functions on the domain of the asymmetry parameter τ, and $\boldsymbol{A} = [a_{ij}]$ is a matrix of coefficients. As described in Schnabel (2011), the coefficients in (9) are estimated with least asymmetrically weighted squares (LAWS) criterion combined with penalized B-splines (P-splines), where the penalty controls the smoothness of the estimates. With a slight modification described by Schnabel and Eilers (2013), the algorithm can be adapted to quantiles as well. The generalized quantile functions $l_\tau(X)$ can be obtained by evaluating $l(X,\tau)$ at a certain level τ. In the following the covariate X used is time of the day and will be denoted by t, such that $l_\tau(X) = l_\tau(t)$.

3.2. Time Series of Functional Data

Electricity demand is recorded in sequential form and shows a similar pattern each day. Naturally, metered demand can be divided into time intervals of 1 day. That is, the deseasonalized time series of metered demand Y_s in (1) is cut into pieces of 1 day, such that each piece consists of the 96 quarter-hourly observations of 1 day. We denote these intradaily load curves as $Y_{t,k}$, where t denotes the time of the day and k denotes the day. Hence, we have two different time dimensions. In the following, when we refer to t we explicitly state time of the day, else we refer to k. We are interested in generalized quantiles of intradaily electricity demand, since they provide information about the distribution of electricity demand. The generalized quantile functions defined in the previous section can be treated as realizations $l_{\tau,k}(t)$ of a functional time series $(l_{\tau,k}, k \in \mathbb{Z})$ defined on a compact set $\mathcal{T}$ and for a fixed $\tau \in (0,1)$. That is, $l_{\tau,k}(t)$ are generalized quantiles of $Y_{t,k}$ and $\mathcal{T}$ corresponds to 1 day. For notational convenience we supress τ in the following, that is, $l_{\tau,k}(t) := l_k(t)$. Under stationarity $l_k(t)$ have a common mean function $\mathrm{E}\{l(t)\} = \mu(t)$ and a common covariance function $C(s,t) = \mathrm{cov}\{l(s), l(t)\}$ with $s, t \in \mathcal{T}$. Note that functional observations are intrinsically infinite dimensional. A common tool to reduce dimensionality is functional principal component analysis (FPCA). For a survey on FPCA, we refer the reader to Shang (2014).

FPCA yields the directions of largest variability in the data and expresses the data as a weighted sum of the orthogonal principal component functions. If $\int_{\mathcal{T}} C(t,t)dt < \infty$, the covariance function induces the Kernel operator $\mathrm{K} : \phi \mapsto \mathrm{K}\phi$ defined by $(\mathrm{K}\phi)(s) = \int_{\mathcal{T}} C(s,t)\phi(t)dt$. Then, C has the representation

$$C(s,t) = \sum_{i=0}^{\infty} \lambda_i\phi_i(s)\phi_i(t), \tag{10}$$

where ϕ_i for $i = 1, 2, \ldots$ are the orthogonal eigenfunctions and λ_i is the corresponding nonincreasing and nonnegative sequence of eigenvalues of the operator K. The eigenfunctions are also called principal component functions. The principal component scores α_i, $i = 1, 2, \ldots$ are given by $\langle l(t), \phi_i\rangle$, where $\langle\cdot,\cdot\rangle$ denotes the inner product. That is, the principal component scores are the projection of $l(t)$ in the direction of the corresponding principal component, with $\mathrm{E}(\alpha_i) = 0$ and $\mathrm{var}(\alpha_i) = \lambda_i$. Using the Karhuhen–Loève expansion, we can express each function $l_k(t)$ as

$$l_k(t) = \mu(t) + \sum_{i=1}^{\infty} \alpha_{ik}\phi_i(t). \tag{11}$$

The functions $l_k(t)$ can be approximated by a finite sum of the first m principal components, called truncated Karhuhen–Loève expansion:

$$l_k(t) \approx \mu(t) + \sum_{i=1}^{m} \alpha_{ik}\phi_i(t). \tag{12}$$

Note that only the principal component scores are varying over time, whereas the mean and principal component functions are time invariant. This observation is exploited for forecasting.

3.3. Estimating FPCA for Generalized Quantiles

In practice, the mean, eigenvalues, and eigenfunctions are unknown and have to be estimated from the sample. The mean of the functions is estimated by

$$\widehat{\mu}(t) = \frac{1}{n}\sum_{k=1}^{n} l_k(t), \tag{13}$$

where n is the sample size. We estimate the kernel operator by

$$(\widehat{\mathrm{K}}\phi)(s) = \int_{\mathcal{T}} \widehat{C}(s,t)\phi(t)dt, \tag{14}$$

where

$$\widehat{C}(s,t) = \frac{1}{n}\sum_{k=1}^{n} \{l_k(s) - \widehat{\mu}(s)\}\{l_k(t) - \widehat{\mu}(t)\}. \tag{15}$$

Estimates of the eigenfunctions and scores are computed from (14) and denoted by $\widehat{\phi}_i$ and $\widehat{\alpha}_{ik}$, $i = 1, \ldots, m$. Hörmann and Kokoszka (2010) showed that these estimates are $\sqrt{n}$-consistent for a large group of stationary functional time series, which includes in particular linear functional processes. To choose the number of principal component functions m in Equation (12) there exist various rules. Here, the number is chosen such that at least an a priori fixed amount of variation in the data is explained by the principal component functions.

3.4. Forecasting Functional Time Series

As noted above, in Equation (11) only the principal component scores α depend on time, while the common mean function μ and the principal component functions ϕ are time-invariant. Hence, the dynamics over time of the generalized quantile curves $l_k(t)$ are fully captured by the dynamics of the principal component scores α. The time dynamics of the first m estimated principal component scores can be modeled using time series analysis (Aue, Norinho, and Hörmann 2015). The problem of modeling the infinite-dimensional functional data objects reduces thus to modeling a multivariate time series.

In our analysis a vector autoregressive model including exogenous variables (VARX) turned out to be suitable to capture the dynamics of the principal component scores. The VARX model of order p is given by

$$\widehat{\boldsymbol{\alpha}}_k = \sum_{i=1}^{p} \boldsymbol{\Phi}_i \widehat{\boldsymbol{\alpha}}_{k-i} + \boldsymbol{\beta}\boldsymbol{x}_k + \boldsymbol{\eta}_k, \tag{16}$$

where $\widehat{\boldsymbol{\alpha}}_k$ is the vector of estimated principal component scores, $\boldsymbol{\Phi}_i$ is a coefficient matrix, $\boldsymbol{x}_k$ are exogenous variables, and $\boldsymbol{\eta}_k$ is a white-noise process (Lütkepohl 2005).

A forecast of the principal component scores directly yields a forecast of the generalized quantile curve:

$$\widehat{l}_{N+h}(t) = \widehat{\mu}(t) + \sum_{i=1}^{m} \widehat{\alpha}_{i,N+h} \widehat{\phi}_i(t), \tag{17}$$

where $\widehat{\alpha}_{i,N+h}$ denotes the h-step ahead forecast of the principal component scores at time N and $\widehat{l}_{N+h}(t)$ is the h-step ahead forecast of the generalized quantile curve. Although suitable here, in a more general setting forecast models for the principal component scores are not restricted to VAR models and can be replaced by many other time series models. The next algorithm summarizes the aforementioned steps:

Algorithm

1. For fixed $\tau \in (0, 1)$ and each $k = 1, \ldots, N$, use the deseasonalized data $Y_{t,k}$, $t = 1, \ldots, 96$ (quarter-hours) to estimate the kth generalized quantile curve $l_{\tau,k}(t)$ by LAWS
2. Fix m and apply FPCA to $l_{\tau,1}, \ldots, l_{\tau,N}$:
   (a) Compute the empirical mean $\widehat{\mu}$, FPCs $\widehat{\phi}_i$ and FPC scores $\widehat{\boldsymbol{\alpha}}_k = (\widehat{\alpha}_{1,k}, \ldots, \widehat{\alpha}_{m,k})^\top$, $k = 1, \ldots, N$, $i = 1, \ldots, m$
3. For fixed h, use the m-variate time series of empirical FPC scores $\widehat{\boldsymbol{\alpha}} = (\widehat{\boldsymbol{\alpha}}_1, \ldots, \widehat{\boldsymbol{\alpha}}_m)^\top$ to obtain h-step ahead forecast $\widehat{\boldsymbol{\alpha}}_{N+h} = (\widehat{\alpha}_{N+h,1}, \ldots, \widehat{\alpha}_{N+h,m})^\top$
   (a) Use a multivariate time series model, for example, VAR model
   (b) Include information from exogenous variables
4. Use $\widehat{\boldsymbol{\alpha}}_{N+h}$ to compute h-step ahead forecast of l_{N+h} as

$$\widehat{l}_{N+h}(t) = \widehat{\mu}(t) + \sum_{i=1}^{m} \widehat{\alpha}_{i,N+h} \widehat{\phi}_j(t)$$

4. Modeling Dynamics of Electricity Demand

As noted above the generalized quantile functions fully characterize the distribution of electricity demand and are an alternative to modeling the distribution function directly. We model the dynamics of the $\tau = 1\%, 5\%, 25\%, 50\%, 75\%, 95\%,$ and 99% expectile functions using the described functional data approach for the 2 years in-sample period from 20100101 to 20113112. The expectile functions are obtained based on the LAWS algorithm, with penalty terms estimated by asymmetric cross-validation. While observed electricity load is usually not smooth, the result from the LAWS algorithm is smooth curves, which can be analyzed using FDA. If one is only interested in point forecasts of electricity load, it is sufficient to estimate expectiles corresponding to $\tau = 0.5$.

Table 2. Explained variance of the first four principal components for the BU Saarbrücken.

	Expectile level τ						
PC	1%	5%	25%	50%	75%	95%	99%
1	0.7221	0.7223	0.7232	0.7195	0.7247	0.7129	0.7233
2	0.1209	0.1213	0.1215	0.1220	0.1199	0.1241	0.1227
3	0.0695	0.0690	0.0687	0.0687	0.0698	0.0691	0.0722
4	0.0394	0.0409	0.0404	0.0420	0.0416	0.0410	0.0409
Total	0.9521	0.9536	0.9540	0.9524	0.9562	0.9572	0.9593

The number of principal components is chosen such that at least 95% of the variation in the data is explained. Tables 2 and 3 show the explained variation of each principal component for all considered expectile levels τ for the BU Saarbrücken and the TSO Amprion, respectively. With four principal components slightly more than 95% of the variation is captured. For all expectile levels, the first PC is the dominant factor, explaining roughly three quarter of the variation in the curves.

To illustrate the results we show the first four principal components for TSO and the BU for $\tau = 0.5$ in Figure 4. For both datasets the extracted PCs exhibit similar shapes. The first principal component reflects variations in the level of electricity load. A positive score on the first principal component implies above average consumption, a negative score below average consumption (see Figure 5 for the scores). The second and third principal components capture variations in the height and location of peak load. The steepness of the load curves is modeled by the fourth principal component.

The load of the TSO is the aggregated load of all BUs located in its area of responsibility. We compare the dynamics of the principal component scores for $\tau = 0.5$ of the TSO and of the BU Saarbrücken to investigate to which degree the quantity risk in the BU is driven by the same factors as the overall market. The scores of the first factor of the TSO and the BU have a correlation of only 0.3 indicating that the level of electricity load of both is only moderately correlated. The correlation of the other scores and different levels of τ is of similar magnitude.

The dynamics of the principal component scores are modeled by a VARX(p) model. The lag order p is chosen by the Akaike information criterion and equals $p = 7$ for all expectile levels. Table 4 shows the estimation results of the exogenous variables for the TSO. Due to limited space, we only display the results for $\tau = 0.05$; 0.5; 0.95. Results for different levels of τ are available from the authors upon request. Note that the values refer to deseasonalized data.

Table 3. Explained variance of the first four principal components for the TSO Amprion.

	Expectile level τ						
PC	1%	5%	25%	50%	75%	95%	99%
1	0.7985	0.7942	0.8007	0.7946	0.7952	0.7956	0.7892
2	0.0878	0.0893	0.0864	0.0883	0.0892	0.0887	0.0920
3	0.0583	0.0586	0.0553	0.0559	0.0547	0.0553	0.0541
4	0.0222	0.0237	0.0240	0.0255	0.0253	0.0252	0.0261
Total	0.9670	0.9659	0.9667	0.9644	0.9645	0.9650	0.9615

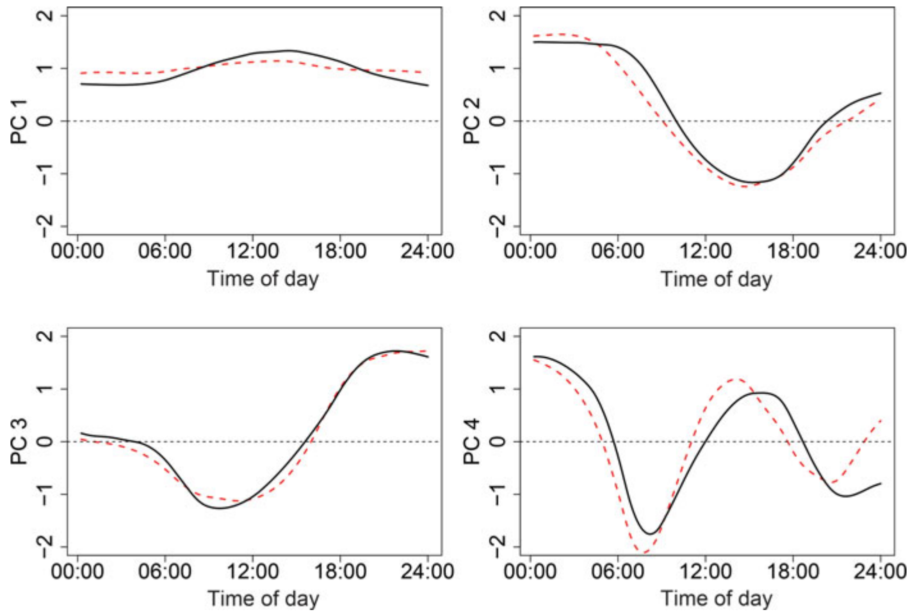

Figure 4. First four principal components corresponding to $\tau = 50\%$ of the TSO Amprion (dashed) and the BU (solid).

Both, daily average temperature and hours of sunshine have a strong negative effect on all four principal component scores, implying that they do not only affect the amount of electricity used, but also the allocation over the day. As expected, an increase in temperature results in lower electricity consumption, since in the area of the TSO Amprion there is a high commonness of electric heating in form of night-storage heaters. Similarly, more hours of sunshine decrease electricity demand, for instance due to less demand for lighting and in-house consumption of solar energy. Peak demand is affected differently by temperature and hours of sunshine as reflected in the sign of the coefficients of the second and third PC score. While higher temperature causes more pronounced peaks, more hours of sunshine flatten the load curve.

For the BU (Table 5), temperature does not have any effect on electricity load. This may be explained by the fact that the share of electric heating is much lower in Saarbrücken than in the total area of the TSO. Therefore, demand is less sensitive to temperature.

To test the validity of our model, a multivariate portmanteau test (Hosking 1980) is performed, which suggests to reject the overall significance of residual autocorrelation for lag orders up to 50.

5. Forecast Evaluation

In this section, we conduct an out-of-sample forecast evaluation using the third year of electricity consumption data (2012) for the BU and the TSO. The forecast evaluation is two-fold. First,

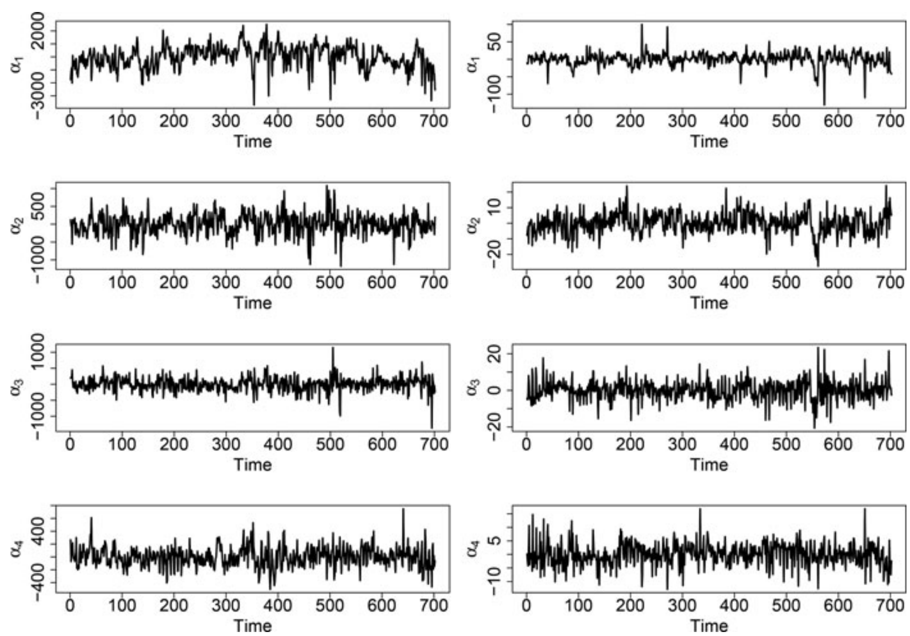

Figure 5. The scores corresponding to the first four principal components for $\tau = 50\%$ of the TSO Amprion (left) and the BU Saarbrücken (right).

Table 4. Estimation results TSO Amprion. Standard deviation in parenthesis.

	α_1	α_2	α_3	α_4
	$\tau = 5\%$			
Temperature	– 22.314***	– 14.805***	– 11.665***	– 3.629**
	(7.175)	(2.903)	(2.620)	(1.564)
Sunshine	– 24.912***	38.058***	20.184***	– 6.308***
	(8.895)	(3.599)	(3.248)	(1.939)
	$\tau = 50\%$			
Temperature	– 22.156***	– 14.708***	– 11.276***	– 3.940**
	(7.141)	(2.896)	(2.591)	(1.576)
Sunshine	– 24.563***	38.198***	20.208***	– 6.059***
	(8.834)	(3.582)	(3.205)	(1.949)
	$\tau = 95\%$			
Temperature	– 21.892***	– 13.771***	– 11.587***	– 3.790**
	(7.187)	(2.930)	(2.593)	(1.557)
Sunshine	– 25.244***	37.850***	21.095***	– 5.633***
	(8.877)	(3.619)	(3.202)	(1.923)

NOTE: $^*p < 0.1$; $^{**}p < 0.05$; $^{***}p < 0.01$.

Table 5. Estimation results BU Saarbrücken. Standard deviation in parenthesis.

	α_1	α_2	α_3	α_4
	$\tau = 5\%$			
Temperature	– 0.038	– 0.039	– 0.016	– 0.039
	(0.154)	(0.058)	(0.054)	(0.041)
Sunshine	– 0.950***	0.633***	0.194***	– 0.204***
	(0.191)	(0.072)	(0.067)	(0.051)
	$\tau = 50\%$			
Temperature	– 0.039	– 0.037	– 0.017	– 0.041
	(0.154)	(0.058)	(0.054)	(0.041)
Sunshine	– 0.958***	0.631***	0.210***	– 0.200***
	(0.190)	(0.072)	(0.067)	(0.051)
	$\tau = 95\%$			
Temperature	– 0.048	– 0.036	– 0.022	– 0.043
	(0.154)	(0.058)	(0.055)	(0.041)
Sunshine	– 0.978***	0.627***	0.228***	– 0.171***
	(0.190)	(0.072)	(0.068)	(0.050)

NOTE: $^*p < 0.1$; $^{**}p < 0.05$; $^{***}p < 0.01$.

we evaluate the results of our approach against well-established methods for electricity demand forecasting. For reasons of comparison, we choose forecasts of the expected value ($\tau = 0.5$) as a reference. Second, we evaluate the quality of the distributional forecasts using an asymmetrically weighted mean squared error criterion.

5.1. Prediction Comparison Methods

To assess the performance of our forecasting approach, we compare it to the results of three different benchmark models. As a first benchmark, we choose the simple Deterministic Seasonal Component (DSC) (Equation (2)). The deterministic seasonal component is straightforward to estimate and in modified forms frequently used in industry. As a further benchmark, we use forecasts that are provided by the TSO Amprion for their area of responsibility. Additionally, we compare our model to the triple seasonal Holt–Winter exponential smoothing (TSHW) model, which was proposed and applied to short-term load forecasting by Taylor (2010). The latter model accommodates yearly, weekly, and daily seasonal cycles and has the advantage that no specification of the functional form is required. Furthermore, Taylor (2010) shows in an application to data from the UK that the TSHW model outperforms simpler exponential smoothing models and performs at least as well as seasonal ARMA models. The formulation of the TSHW model is given by

$$\begin{aligned}\widehat{l}_{s+h} &= g_s + d_{s-c_1+h} + w_{s-c_2+h} + a_{s-c_3+h} \\ &\quad + \phi^h (l_s - g_{c-1} - d_{s-c_1} - w_{s-c_2} - a_{s-c_3}) \quad (18)\\ g_s &= \alpha (l_s - d_{s-c_1} - w_{s-c_2} - a_{s-c_3}) + (1-\alpha) g_{s-1} \quad (19)\\ d_s &= \delta (l_s - g_s - w_{s-c_2} - a_{s-c_3}) + (1-\delta) d_{s-c_1} \quad (20)\\ w_s &= \omega (l_s - g_s - d_{s-c_1} - a_{s-c_3}) + (1-\omega) w_{s-c_2} \quad (21)\\ a_s &= \lambda (l_s - g_s - d_{s-c_1} - w_{s-c_2}) + (1-\lambda) a_{s-c_2}, \quad (22)\end{aligned}$$

where $\widehat{l}_{s+h}$ denotes the h-step ahead load forecast at time s, g_s is the smoothed load, and d_s, w_s, and a_s are seasonal indices for daily, weekly, and annual cycles, with c_1, c_2, c_3 denoting the length of the respective cycles. $\alpha, \delta, \omega, \lambda$ are smoothing parameters and the term including ϕ is an adjustment for first-order autocorrelation. Note that in this model, quarter-hourly forecasts for 1 day correspond to a forecast horizon of 96. For the forecast evaluation, we reshape the results analogously to the time series of metered demand (see Section 3.2).

5.2. Forecast Results

The performance of the different forecasting methods is evaluated based on the root mean squared error (RMSE) defined as

$$\text{RMSE}_h = \sqrt{\frac{1}{96} \sum_{t=1}^{96} \left\{ Y_{t,N+h} - \widehat{l}_{N+h}(t) \right\}^2} \quad (23)$$

and the mean absolute percentage error (MAPE) given by

$$\text{MAPE}_h = \frac{1}{96} \sum_{t=1}^{96} \left| \frac{Y_{t,N+h} - \widehat{l}_{N+h}(t)}{\widetilde{Y}_{t,N+h}} \right|, \quad (24)$$

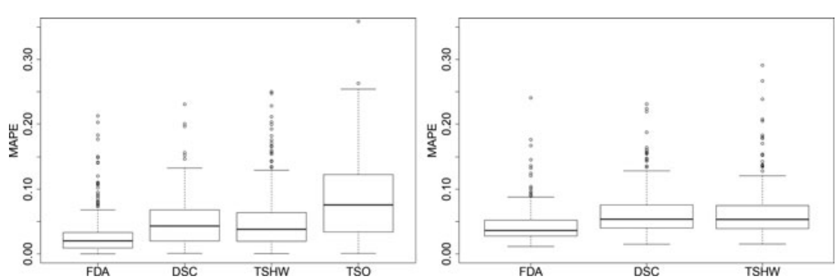

Figure 6. Boxplot of the mean absolute percentage forecasting error for the TSO (left) and the BU (right) of the functional data approach (FDA), the deterministic seasonal component (DSC), the triple seasonal Holt–Winter exponential smoothing model (TSHW), and the forecast provided by the transmission system operator (TSO).

Table 6. Mean of RMSE and MAPE for the TSO and the BU of functional data approach (FDA) with $\tau = 0.5$, deterministic seasonal component (DSC), triple seasonal Holt–Winter exponential smoothing (TSHW), and forecast provided by the transmission system operator (TSO).

	FDA	DSC	TSHW	TSO
		TSO		
RMSE	711.72	1021.16	932.81	3064.97
MAPE	0.027	0.045	0.043	0.13
		Balancing unit		
RMSE	23.16	30.30	34.71	—
MAPE	0.043	0.062	0.066	—

where $h = 1, \ldots, H$ denotes the day-ahead forecasts and $\widehat{l}_{N+h}(t)$ is the forecasted expected load on day $N + h$ and time of day t. Table 6 reports the mean of the RMSE and MAPE based on $H = 351$ out-of-sample day-ahead forecasts over the year 2012. Meteorological forecasts of the explanatory variables are used as covariates. The proposed methodology clearly outperforms the benchmark models in terms of the given measures. Surprisingly, also the simple DSC performs relatively well and yields results similar to those of the TSHW exponential smoothing model. This underlines the very regular structure in intradaily electricity consumption. Figure 6 shows boxplots of the MAPE. The distribution of MAPE of the FDA is most narrow, however it contains several extreme values at the right tail. Overall, the figures indicate that our model performs quite well in point forecasting and results in forecasts with an average absolute deviation of only 2.7% for the TSO and 4.3% for the BU.

To evaluate the performance of the distributional forecasts, we look at the accuracy of the expectile estimates for $\tau = 0.01, 0.05, 0.25, 0.75, 0.95, 0.99$. As pointed out by Guler, Ng, and Xiao (2014), a performance measure should be used that reflects the asymmetric loss function of expectiles. We choose the root mean weighted squared error (RMWSE) defined as

$$\mathrm{RMWSE}_h^\tau = \sqrt{\frac{1}{96}\sum_{t=1}^{96}\left|\tau - \mathrm{I}_{\{Y_{t,N+h}<\widehat{l}_{\tau,N+h}(t)\}}\right|\left\{Y_{t,N+h} - \widehat{l}_{\tau,N+h}(t)\right\}^2}, \quad (25)$$

where $\widehat{l}_{\tau,N+h}(t)$ denotes the forecasted τ-expectile of electricity load on day $N + h$ and time of day t. Summary statistics of the RMWSE for the different expectile levels based on $H = 351$ day-ahead forecasts are given in Table 7. The results indicate high precision of the estimated tail curves. Figure 7 shows a plot of the forecasted mean (black line) together with forecast intervals corresponding to various expectile levels (gray shades) and the observed load for the TSO Amprion. The intervals spanned by the expectile curves provide information about the dispersion and asymmetry of next day's load. Furthermore, as pointed out above, quantiles and expectiles can be optimal point forecasts if the forecasters' loss function is asymmetric. In energy demand forecasting, asymmetric loss functions occur if the cost for positive and negative imbalance is asymmetric, as it is the case in Scandinavian countries (Linnet 2005). In that case, trading strategies based on quantiles and expectiles can be beneficial.

Table 7. Summary statistics of RMWSE.

	Expectile level τ						
	1%	5%	25%	50%	75%	95%	99%
				TSO			
Mean	566.83	685.42	700.51	711.72	673.97	611.88	496.68
SD	440.98	494.81	420.20	416.40	391.32	432.82	373.50
				BU			
Mean	13.93	16.82	20.90	23.16	24.47	24.20	23.36
SD	6.57	6.71	6.49	7.61	9.31	10.93	11.41

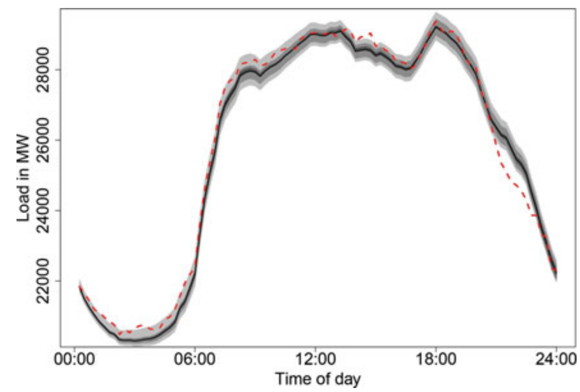

Figure 7. Forecasted expected load (black solid line) together with forecasts of $\tau = 0.01, 0.05, 0.25, 0.75, 0.95, 0.99$ expectiles (gray shades) and observed load (red dashed line) for TSO Amprion on 20120125.

6. Conclusion

In this article, we show how to get powerful probabilistic short-term forecasts of intradaily electricity load employing functional data analysis methods with generalized quantile regression. Probabilistic forecasts yield important information about the uncertainty of future demand and are crucial for sustainable operation of electric utilities and for traders in the electricity market. This novel approach has several advantages: It allows for flexible inclusion of explanatory variables and does not require distributional assumptions for neither the tails nor the functional form of the time-varying curves. The empirical analysis is based on quarter-hourly data from a TSO and a BU in western Germany. The proposed methodology identifies the main risk drivers of the electricity load by a number of factors: variations in the level of electricity load, variation in the height and location of peak load, and the steepness of the load curves. We show how these factors are then to be (cor)related with climate effects.

In a forecast comparison study, we find that our methodology outperforms real forecasts (an MAPE of 2.7%) provided by the TSO as well as those of the benchmark models.

Supplementary Materials

Simulation Study: A simulation study that evaluates the performance of the proposed methodology. The results are compared to several benchmark methods. (PDF)

Funding

The financial support from the Deutsche Forschungsgemeinschaft via SFB 649 "Ökonomisches Risiko," Humboldt-Universität zu Berlin is gratefully acknowledged.

References

Aneiros, G., Cao, R., Vilar-Fernández, J. M., and Muñoz-San-Roque, A. (2011), "Functional Prediction for the Residual Demand in Electricity Spot Markets," in *Recent Advances in Functional Data Analysis and Related Topics*, ed. F. Ferraty, New York: Springer, pp. 9–15. [128]

Antoch, J., Prchal, L., De Rosa, M. R., and Sarda, P. (2008), "Functional Linear Regression With Functional Response: Application to Prediction of Electricity Consumption," in *Functional and Operatorial Statistics*, eds. S. Dabo-Niang and F. Ferraty, New York: Springer, pp. 23–29. [128]

Aue, A., Norinho, D. D., and Hörmann, S. (2015), "On the Prediction of Stationary Functional Time Series," *Journal of the American Statistical Association*, 110, 378–392. [131]

Bellini, F., Klar, B., Müller, A., and Rosazza-Gianin, E. (2014), "Generalized Quantiles as Risk Measures," *Insurance: Mathematics and Economics*, 54, 41–48. [127,130]

Bremnes, J. B. (2004), "Probabilistic Wind Power Forecasts Using Local Quantile Regression," *Wind Energy*, 7, 47–54. [127]

Cho, H., Goude, Y., Brossat, X., and Yao, Q. (2013), "Modeling and Forecasting Daily Electricity Load Curves: A Hybrid Approach," *Journal of the American Statistical Association*, 108, 7–21. [128]

Cottet, R., and Smith, M. (2003), "Bayesian Modeling and Forecasting of Intraday Electricity Load," *Journal of the American Statistical Association*, 98, 839–849. [127]

Engel, R. F., Granger, C. W. J., Rice, J., and Weiss, A. (1986), "Semiparametric Estimated of the Relation Between Weather and Electricity sales," *Journal of the American Statistical Association*, 81, 310–320. [128,129]

EPEX Spot. (2014), "EPEX Spot Annual Report 2013," available at *https://www.epexspot.com/document/28679/EPEX 02013.pdf* [128]

Eurostat. (2014), "Supply, Transformation, Consumption - Electricity - Annual Data," available at *http://epp.eurostat.ec.europa.eu* [128]

Ferraty, F., Goia, A., Salinelli, E., and Vieu, P. (2014), "Peak-Load Forecasting Using a Functional Semi-Parametric Approach," in *Topics in Nonparametric Statistics*, eds. M. G. Akritas, S. N. Lahiri, D. N. Politis, New York: Springer, pp. 105–114. [128]

Ferraty, F., and Vieu, P. (2006), *Nonparametric Functional Data Analysis: Theory and Practice*, New York: Springer. [130]

Gneiting, T. (2011), "Quantiles as Optimal Point Forecasts," *International Journal of Forecasting*, 27, 197–207. [127]

Goia, A., May, C., and Fusai, G. (2010), "Functional Clustering and Linear Regression for Peak Load Forecasting," *International Journal of Forecasting*, 26, 700–711. [128]

Guler, K., Ng, P. T., and Xiao, Z. (2014), "Mincer-Zarnovitz Quantile and Expectile Regressions for Forecast Evaluations under Asymmetric Loss Functions," Working Paper Series No. 14-01, Northern Arizona University. [135]

Guo, M., Zhou, L., Härdle, W. K., and Huang, J. Z. (2015), "Functional Data Analysis of Generalized Regression Quantiles," *Statistics and Computing*, 25, 189–202. [128]

Harvey, A., and Koopman, S. J. (1993), "Forecasting Hourly Electricity Demand Using Time-Varying Splines," *Journal of the American Statistical Association*, 88, 1228–1236. [128]

Hörmann, S., and Kokoszka, P. (2010), "Weakly Dependent Functional Data," *The Annals of Statistics*, 38, 1845–1884. [128,131]

Horváth, L., and Kokoszka, P. (2012), *Inference for Functional Data with Applications*, New York: Springer. [128]

Hosking, J. R. (1980), "The Multivariate Portmanteau Statistic," *Journal of the American Statistical Association*, 75, 602–608. [133]

Hyndman, R. J., and Fan, S. (2010), "Density Forecasting for Long-Term Peak Electricity Demand," *IEEE Transactions on Power Systems*, 25, 1142–1153. [127]

Jones, M. C. (1994), "Expectiles and M-Quantiles are Quantiles," *Statistics & Probability Letters*, 20, 149–153. [130]

Koenker, R. (2005), *Quantile Regression*, Cambridge, UK: Cambridge University Press. [130]

Koenker, R., and Bassett Jr, G. (1978), "Regression Quantiles," *Econometrica: Journal of the Econometric Society*, 46, 33–50. [127]

Leutbecher, M., and Palmer, T. (2008), "Ensemble Forecasting," *Journal of Computational Physics*, 227, 3515–3539. [127]

Liebl, D. (2013), "Modeling and Forecasting Electricity Spot Prices: A Functional Data Perspective," *The Annals of Applied Statistics*, 7, 1562–1592. [128]

Linnet, U. (2005), "Tools Supporting Wind Energy Trade in Deregulated Markets," Ph.D. dissertation, Technical University of Denmark. [135]

Lütkepohl, H. (2005), *New Introduction to Multiple Time Series Analysis*, New York: Springer. [132]

Mayer, J. (2014), "Electricity Production and Spot-Prices in Germany 2014," available at *https://www.ise.fraunhofer.de/en/downloads-englisch/pdf-files-englisch/data-nivc-/electricity-spot-prices-and-production-data-in-germany-2014.pdf* [128]

Newey, W. K., and Powell, J. L. (1987), "Asymmetric Least Squares Estimation and Testing," *Econometrica: Journal of the Econometric Society*, 55, 819–847. [127,130]

Pinson, P., Chevallier, C., and Kariniotakis, G. N. (2007), "Trading Wind Generation from Short-Term Probabilistic Forecasts of Wind Power," *IEEE Transactions on Power Systems*, 22, 1148–1156. [127]

Ramsay, J. O., and Silverman, B. W. (2002), *Applied Functional Data Analysis: Methods and Case Studies*, New York: Springer. [130]

——— (2005), *Functional Data Analysis*, New York: Springer. [128]

Schnabel, S. (2011), "Expectile Smoothing: New Perspectives on Asymmetric Least Squares. An Application to Life Expectancy," Ph.D. dissertation, Utrecht University. [130,131]

Schnabel, S. K., and Eilers, P. H. C. (2013), "Simultaneous Estimation of Quantile Curves using Quantile Sheets," *AStA Advances in Statistical Analysis*, 97, 77–87. [131]

Shang, H. L. (2013), "Functional Time Series Approach for Forecasting Very Short-Term Electricity Demand," *Journal of Applied Statistics*, 40, 152–168. [128]

——— (2014), "A Survey of Functional Principal Component Analysis," *AStA Advances in Statistical Analysis*, 98, 121–142. [131]

Tay, A. S., and Wallis, K. F. (2000), "Density Forecasting: A Survey," *Journal of Forecasting*, 19, 235–254. [127]

Taylor, J. W. (2008), "Estimating Value at Risk and Expected Shortfall Using Expectiles," *Journal of Financial Econometrics*, 6, 231–252. [127]

——— (2010), "Triple Seasonal Methods for Short-Term Electricity Demand Forecasting," *European Journal of Operational Research*, 204, 139–152. [134]

Taylor, J. W., and Buizza, R. (2002), "Neural Network Load Forecasting with Weather Ensemble Predictions," *IEEE Transactions on Power Systems*, 17, 626–632. [129]

Taylor, J. W., and McSharry, P. E. (2007), "Short-Term Load Forecasting Methods: An Evaluation Based on European Data," *IEEE Transactions on Power Systems*, 22, 2213–2219. [127,128]

Tran, N. M., Osipenko, M., and Härdle, W. K. (2016), "Principal Component Analysis in an Asymmetric Norm," CRC 649 Discussion Paper 2016-040, Humboldt University, Berlin. [128]

Vilar, J. M., Cao, R., and Aneiros, G. (2012), "Forecasting Next-Day Electricity Demand and Price using Nonparametric Functional Methods," *International Journal of Electrical Power & Energy Systems*, 39, 48–55. [128]

Weron, R. (2007), *Modeling and Forecasting Electricity Loads and Prices: A Statistical Approach*, New York: Wiley. [127]